BRNO UNIVERSITY OF TECHNOLOGY

FACULTY OF ELECTRICAL ENGINEERING
AND COMMUNICATION

DEPARTMENT OF TELECOMMUNICATIONS

Ing. Michaela Novosadová

IMAGE EDGE DETECTION USING CONVEX OPTIMISATION

DETEKCE HRAN V OBRAZE POMOCÍ KONVEXNÍ OPTIMALIZACE

SHORTENED VERSION OF PH.D. THESIS

Specialization: Teleinformatics

Supervisor: prof. Mgr. Pavel Rajmic, Ph.D.

Opponents:

Date of Defense:

KEYWORDS

Signal segmentation, image edge detection, convex optimisation, proximal splitting algorithm, proximal operator, sparsity, total variation, gradient

KLÍČOVÁ SLOVA

Segmentace signálů, detekce hran v obraze, konvexní optimalizace, proximální algoritmy, proximální operátory, řídkost, totální variace, gradient

ARCHIVED IN

Dissertation is available at the Science Department of Dean's Office FEEC, Brno University of Technology, Technická 10, Brno, 616 00

MÍSTO ULOŽENÍ PRÁCE

Disertační práce je k dispozici na Vědeckém oddělení děkanátu FEKT VUT v Brně, Technická 10, Brno, 616 00

© Michaela Novosadová, 2023

ISBN 80-214-

ISSN 1213-4198

CONTENTS

INTRODUCTION

Sparse representation has proven to be a very powerful tool in a variety of applications, especially in signal processing, image processing, machine learning, and computer vision. The list of specific tasks concerning images, for which sparse representation offers a huge potential, contains image inpainting, image denoising, image segmentation, visual tracking, and more. Another example of a popular topic in the last few years, where the use of sparse representation is definitely beneficial and favourable, is image classification. Sparse representation are directly related to compressed sensing, which can be seen as a method for recovering a sparse signal from a small number of linear measurements.

Specific problems of the mentioned topics, which need to be solved, can be often represented via convex optimisation problems. Searching for the sparse representation contributed to the development of numerical methods for solving convex optimisation problems – specifically the proximal algorithms, which are iterative algorithms based on the evaluation of the proximal operators associated with the optimised function. Optimisation problems can be solved using approximation algorithms, which can be divided into three categories: the greedy algorithms, relaxation algorithms (which include also the proximal algorithms) and "hybrid" algorithms, combining different approaches.

The image edge detection is one of the most used techniques in digital image processing, computer and robot vision. It finds application in many topics such as object tracking, motion detection, pattern recognition, image segmentation, medical data processing, etc. An edge in the image is usually defined as a position where the intensity of an image changes significantly. However, each application requires a different estimation of what a significant edge is and thus there are several different approaches suited for each application.

Image edge detection can be viewed as the first step of image segmentation, therefore, even nowadays, the edge detection is in the focus of researchers who are still trying to develop better edge detection techniques.

Image segmentation is one of the most important applications in digital signal processing. Segmentation divides an image into areas (segments) which have similar features or form logical parts. These segments are disjoint and cover the entire image. A very interesting and important area of image segmentation is a segmentation of medical images.

The most frequently used imaging modalities for anatomical structure imaging in medicine are Computed Tomography (CT), Magnetic Resonance (MR) and Ultrasound. Image segmentation is most often applied to CT and MR images. These imaging modalities are used for diagnostic and treatment planning in various medical disciplines. In the time of developing 3D printing, the importance of image segmentation is increasing. Doctors can print segmented organs on a 3D printer and plan the operation on anatomical models of a particular patient.

This Thesis works with an assumption that an image can be modelled as an overcomplete piecewise polynomial image, such as the image consisting of disjoint piecewise-polynomial patches/segments. The number of the signal segments S is considerably lower than the number of the signal samples N ($S \ll N$), which motivates to measure and optimise sparsity in

parametrisation images. Based on the above-mentioned assumptions, the convex recovery problem can be formulated.

Our approach was inspired by authors of [11], who used a greedy approach to solve the optimisation problem for signal segmentation. The presented approach is using the over-parametrisation signal model and ℓ_1-based convex relaxation methods. To the best of our knowledge, it is the first time when the ℓ_1 minimisation-based approach is used for signal segmentation/edge detection.

First, the convex optimisation problems for one-dimensional signal segmentation and denoising are formulated since it is easier to implement appropriate algorithms able to solve such formulated problems, and determine their advantages and disadvantages for one-dimensional signals than for two-dimensional signals, i.e. images. Afterwards, the formulation of the convex optimisation problem for the image edge detection, later solved by the most promising algorithm from the 1D segmentation phase, takes place.

1 THEORY

1.1 Sparse representation

In the beginning, the term "sparse" should be clarified. It can be used to describe the properties of a matrix or a vector, which can be called sparse if most of its elements are zero [12].

The term "sparse" can be also used to describe the properties of a signal representation. The representation of a signal is sparse if the signal is modelled as a linear combination of only a few elements from the dictionary $\mathbf{A}$. The dictionary consists of a set of basis elements (called atoms) and it is always formed with respect to a specific task [13]. Sparse representation is important for many applications [12]. The advantages of sparse representations include simplifying the interpretation of data, enabling easy and strong compression or providing numerical stability.

The intention of the sparse-based methods is to select a few atoms from the dictionary that best represent given signal $\mathbf{y} \in \mathbb{R}^N$. Signal $\mathbf{y}$ is defined by the linear system $\mathbf{y} = \mathbf{A}\mathbf{x}$, where $\mathbf{A} \in \mathbb{R}^{N \times M}$ is the dictionary and $\mathbf{x} \in \mathbb{R}^N$ is the parametrisation vector with parametrisation coefficients [14]. The aim is to find a sparse solution of the given linear system with as few parametrisation coefficients as possible.

Sparsity k of the solution concerns the number of non-zero coefficients in a vector of length N. The sparsity is usually measured by the ℓ_0-norm, which refers to the number of non-zero entries k. A vector is called k-sparse, when its ℓ_0-norm is equal to k. Usually, it holds that $k < N$ or $k \ll N$ [15].

The basic sparse representation problem is formulated as:

$$\arg\min_{\mathbf{x}} \|\mathbf{x}\|_0 \quad \text{s.t.} \quad \mathbf{A}\mathbf{x} = \mathbf{y}. \tag{1.1}$$

The problem is NP-hard and the solution is difficult to approximate. The ℓ_0-norm is a non-convex function and therefore, it is not possible to use any of the algorithms of convex optimisation for solving the problem (1.1). To be able to use the convex optimisation, it is necessary to use convex ℓ_p-norms, which are convex for $p \geq 1$.

In the case of noisy signal $\mathbf{y}$, defined as $\mathbf{y} = \mathbf{A}\mathbf{x}+\mathbf{e}$, where $\mathbf{e} \in \mathbb{R}^N$ is noise, the optimisation problem can be recast to:

$$\arg\min_{\mathbf{x}} \|\mathbf{x}\|_1 \quad \text{s.t.} \quad \|\mathbf{A}\mathbf{x} - \mathbf{y}\|_2 \leq \delta, \tag{1.2}$$

where δ is a noise level. It will be shown later that for finding the solution to the optimisation problem (1.2), the convex optimisation can be used.

1.2 Convex optimisation

In mathematics, computer science, and economics, an optimisation problem is determined by finding the best solution among all possible solutions. A general optimisation problem can be defined as follows [16]:

$$\text{minimise} \quad f_0(\mathbf{x}) \quad \text{s.t.} \quad f_i(\mathbf{x}) \leq \delta_i, \quad i = 1, \ldots, m, \tag{1.3}$$

where $\mathbf{x}$ is the optimisation variable of the problem, f_0 is the objective function, f_i are constraint functions, and δ_i are limits of the constraints. The solution to the optimisation problem (1.3) is the vector $\hat{\mathbf{x}}$ producing the smallest objective value among all vectors satisfying the constraints, i.e. for any $\mathbf{z}$ with $f_1(\mathbf{z}) \leq \delta_1, \ldots, f_m(\mathbf{z}) \leq \delta_m$, it holds $f_0(\mathbf{z}) \geq f_0(\hat{\mathbf{x}})$.

1.3 Proximal splitting algorithms

Proximal splitting algorithms (PAs) are in general able to solve unconstrained convex optimisation problems of type

$$\arg\min_{\mathbf{x}} f_1(L_1\mathbf{x}) + \cdots + f_m(L_m\mathbf{x}), \tag{1.4}$$

where functions $f_1, \ldots, f_m$ are convex and $L_1, \ldots, L_m$ are linear operators [17]. Note, however, that some algorithms are restricted regarding the number of minimised functions and linear operators. For instance, the Douglas–Rachford algorithm is able to find the minimum of the sum of only two convex functions, without linear operators (i.e. the linear operators are identities).

The PAs are suitable for finding the minimum of a sum of convex functions during an iterative process. A process of iterations is generally terminated after a pre-defined number of iterations or if a convergence criterion is met, e.g. the change in the solution is small enough: $\|\hat{\mathbf{x}}^{i+1} - \hat{\mathbf{x}}^i\|_2 / \|\hat{\mathbf{x}}^i\|_2 \leq \varepsilon$, where i is the number of the iteration and ε is the parameter of the convergence criterion. Proximal splitting algorithms are proven to provide convergence to the optimal value. However, in practice, convergence and its speed are greatly affected by the nature of the functions and parameters used in the algorithm.

The PAs perform iterations involving the evaluation of gradients and/or proximal operators (see below) related to individual functions, which is much simpler than minimisation of the composite functional by other means. The advantage of proximal splitting algorithms is that they allow solving the minimisation problems even with non-smooth functions. Each non-smooth function is involved via its proximity operator.

Several proximal splitting algorithms exist, and their application depends on the definition of the minimisation problem. In this Thesis, these proximal splitting algorithms are used: the Forward-backward (FB) algorithm [17], the Douglas–Rachford (DR) algorithm [17], the Chambolle–Pock (CP) algorithm [18], the Forward-backward based primal-dual (FBB-PD) algorithm [19], and the Condat algorithm [20, 21].

1.4 Edge detection

An edge is defined as a position in the image where it is a significant local change in the image intensity. A stronger change of the intensity causes clearer edge, which can be detected more easily and more precisely. Edges provide important visual information, for example each object can be easily described with few key edges and therefore, edges are important for human sight.

Edge detection can be interpreted as a transformation of the grayscale or colour image to the binary image, where white pixels represent the edge position and black pixels represent the background or vice versa. Finding the place where the change in the image intensity is strong, is the appropriate way how to find the edges. Many approaches to the edge detection were designed. An easy and very common approach to the edge detection is application of the edge operators.

Edge strength and orientation An edge can be described by their strength and orientation. Edge strength and orientation are computed from the results of the convolution of the original image with the gradient masks for each image position. [22, 23]

Edge detection and noise The result of the edge detection is significantly affected by noise in the image, which usually causes the detection of false edges. This phenomena is naturally more significant with stronger noise and in the case of simple edge detection methods. These false detected edges should be excluded via post-processing, which takes image context into consideration. [22]

Edge maps The result of the edge detection approach is full of edge candidates. The decision on which candidate is truly an edge and which is not is a very important part of the post-processing. The simplest method to decide this is to apply thresholding to the edge strength. The threshold value can be fixed or adaptive. The decision process leads to the binary image – so called edge map. [23]

1.5 Denoising

Denoising or noise smoothing can be viewed as a signal enhancement, which focuses on the compensation of the signal imperfections caused by the noise, providing the assumption of the original "clean" signal [22]. Noise smoothing is realised mostly by local operators (masks) – linear or non-linear and space invariant or adaptive.

An image can be corrupted by a different kind of noise. The origin of the noise plays important role in choosing the suitable noise-suppressing method.

2 THESIS AIMS AND OBJECTIVES

The main aim of the Thesis is to propose, implement, and evaluate an effective method for image edge detection.

To do this, the first step is to propose a suitable convex optimisation problem that can deal with the problem of edge detection. Since there are many methods for solving convex optimisation problems, appropriate optimisation algorithms will be chosen to solve the problem numerically.

The authors of [11] used greedy approach to solve the optimisation recovery problem for signal segmentation. Inspired by this work, the intent of this Thesis is to explore how the ℓ_1-based convex relaxation methods will deal with the recovery problems for 1D signal segmentation and denoising. To the best of our knowledge, it will be the first time when the ℓ_1 minimisation-based approach will be used for signal segmentation/breakpoint detection.

First, the convex optimisation problems for one-dimensional signal segmentation and denoising will be formulated. It is easier to formulate the recovery problems, implement appropriate algorithms able to solve such formulated problems, and determine their advantages and disadvantages for one-dimensional signals than for 2D signals, i.e. images.

One of the advantages of the the 1D case is that segmentation and denoising are performed simultaneously. Denoising can be considered as a side-product of this solution. Furthermore, each detected segment can be denoised separately once again, to obtain a better denoising effect.

The first step will be to compare these methods on 1D signals, and then the method that gives the most promising results on 1D signals will be extended for the use in the higher dimension. Afterwards, the convex optimisation problems for the detection of edges in images will be formulated, which will be then solved by the most promising algorithm from the 1D segmentation phase.

A necessary part of the Thesis is the evaluation of the obtained results, which will be performed on a generated dataset of 1D synthetic signals and a public image dataset (BSDS500). Several evaluation metrics described in the Thesis will be used to evaluate the results on 1D and 2D signals.

Following the idea of reproducible research, the implementations of the algorithms for 1D signal segmentation and denoising and for image edge detection will be made publicly available.

All the chosen algorithms will be implemented in Matlab, some proximal algorithms for convex optimisation will be implemented using the UnLocBox toolbox[24].

A repository of Matlab implementations of the developed 1D signal segmentation and denoising algorithms and image edge detection algorithm will be created, including also the test datasets of 1D signals, images, and bases.

3 SEGMENTATION OF 1D SIGNALS

3.1 Test signals and bases, evaluation

For the experiments, test datasets of synthetic signals and bases are created. The dataset of synthetic signals is in this Thesis represented by the group of piecewise-linear and piecewise-quadratic signals.

Synthetic signals As elementary signals for creating a dataset of linear signals, 10 random piecewise-linear signals $\mathbf{y}_{\text{clean}}$ ($K = 1$) with 6 signal segments ($S = 6$), and without jumps of length $N = 300$ are generated. For each elementary signal, 10 variations of the signal with $L = 10$ levels of the jump height $\mathbf{h} = [h_1, \ldots, h_{10}]$ are generated. Five SNR values are prescribed for the experiments: 15, 20, 25, 30, and 35 dB. For each signal and each SNR, 50 realizations of noise are generated, making a set of 27,500 noisy signals $\mathbf{y}$ in total. Examples of clean linear signals $\mathbf{y}_{\text{clean}}$ are depicted in Fig. 3.1a.

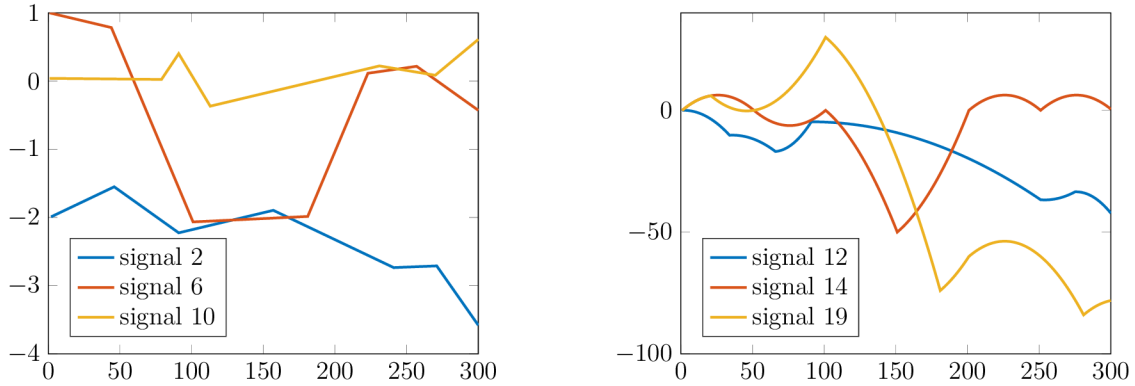

(a) Synthetic piecewise-linear signals

(b) Synthetic piecewise-quadratic signals

Fig. 3.1: Examples of used synthetic piecewise-linear and piecewise-quadratic signals. The left-hand side figure shows the examples of used clean synthetic piecewise-linear signals – signal 2, 6, and 10. The right-hand side figure shows the examples of used clean synthetic piecewise-quadratic signals – signal 12, 14, and 15.

The dataset of piecewise-quadratic signals is created with the same process as the dataset of piecewise-linear signals, with one difference. At the beginning, 10 randomly piecewise-quadratic signals $\mathbf{y}_{\text{clean}}$ (K=2) are generated, instead of the set of 10 randomly generated piecewise-linear signals. Examples of clean quadratic signals $\mathbf{y}_{\text{clean}}$ are depicted in Fig. 3.1b.

Bases In this Thesis, the bases are divided into groups according to their orthogonality and normalisation. All the polynomial bases consist of $K + 1$ basis vectors, which are linearly independent discrete-time polynomials $\mathbf{p}_k$. The basis vectors $\mathbf{p}_k$ can be viewed as the columns of the $N \times (K + 1)$ matrix and they form the diagonals of the matrix $\mathbf{P}$ in the model (3.1). According to the properties of the particular polynomials, the bases can be divided into:

modified standard basis **S**, non-orthogonal bases **B**, normalised bases **N**, orthogonal bases **O**, and random orthogonal bases **R**. The modified standard basis **S** and example of the O-basis are shown in Fig. 3.2. For most of the experiments, only the modified standard basis **S** is used. Then only the groups of the O-bases and R-bases are generated and used in this Thesis, where each group consists of 20 particular bases.

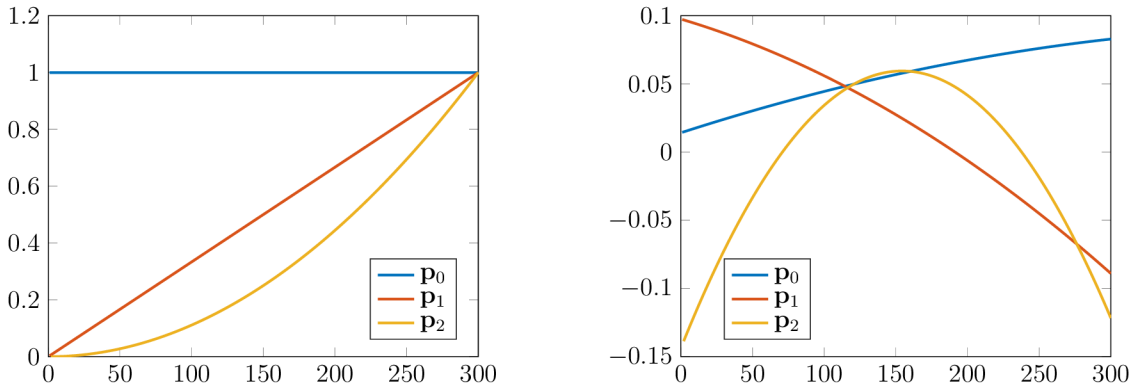

(a) Modified standard basis.

(b) O-basis.

Fig. 3.2: The modified standard basis **S** and O-basis **O** consisting of three basis polynomials.

Evaluation

Two points of view are used for the evaluation of the results of the 1D signal segmentation and denoising process. The first one is evaluation of the quality of signal segmentation, i.e. breakpoint detection accuracy. The second one is the evaluation of obtained signal denoising.

For such an evaluation, several metrics are used - AAR, MMR, and NoB for breakpoint detection accuracy, and SNR and MSE for denoising performance. The most important evaluation parameter for breakpoint detection accuracy is the number of correctly detected breakpoints (NoB), for denoising performance, it is signal-to-noise ratio (SNR).

3.2 Signal model description

A signal $\mathbf{y}$ can be modelled as

$$\mathbf{y} = \mathbf{P}\mathbf{x} = \left[\mathbf{P}_0 \mid \cdots \mid \mathbf{P}_K\right] \begin{bmatrix} \mathbf{x}_0 \\ \hline \vdots \\ \hline \mathbf{x}_K \end{bmatrix} = \mathbf{p}_0 \odot \mathbf{x}_0 + \cdots + \mathbf{p}_K \odot \mathbf{x}_K, \tag{3.1}$$

where the length of $\mathbf{x}$ is $(K+1)N$ and $\mathbf{P}$ is a fat matrix of size $N \times (K+1)N$, $\odot$ denoting the elementwise (Hadamard) product. Signal $\mathbf{y}$, parametrisation vectors $\mathbf{x}_k$, polynomial bases

$\mathbf{p}_k$ and matrices $\mathbf{P}_k$ (for $k = 0, \ldots, K$) are defined as

$$\mathbf{y} = \begin{bmatrix} y[1] \\ \vdots \\ y[N] \end{bmatrix}, \quad \mathbf{x}_k = \begin{bmatrix} x_k[1] \\ \vdots \\ x_k[N] \end{bmatrix}, \quad \mathbf{p}_k = \begin{bmatrix} p_k[1] \\ \vdots \\ p_k[N] \end{bmatrix}, \quad \mathbf{P}_k = \mathrm{diag}(\mathbf{p}_k) = \begin{bmatrix} p_k[1] & & 0 \\ & \ddots & \\ 0 & & p_k[N] \end{bmatrix}. \tag{3.2}$$

Such a description of a N-dimensional signal is obviously overcomplete in terms of the number of parameters. When the polynomials in $\mathbf{P}$ are fixed, $(K+1)N$ parameters are used to characterise the signal.

Nevertheless, it is assumed that $\mathbf{y}$ is piecewise-polynomial and that it consists of S independent segments. Each segment $s \in \{1, \ldots, S\}$ is then described by $K+1$ basis polynomials. This can be achieved by letting all the vectors $\mathbf{x}_k$ be piecewise-constant within the particular segments, with the change at the segment borders. See Fig. 3.3 for illustration. The positions of the segment borders are unknown and they will be the subject of the search.

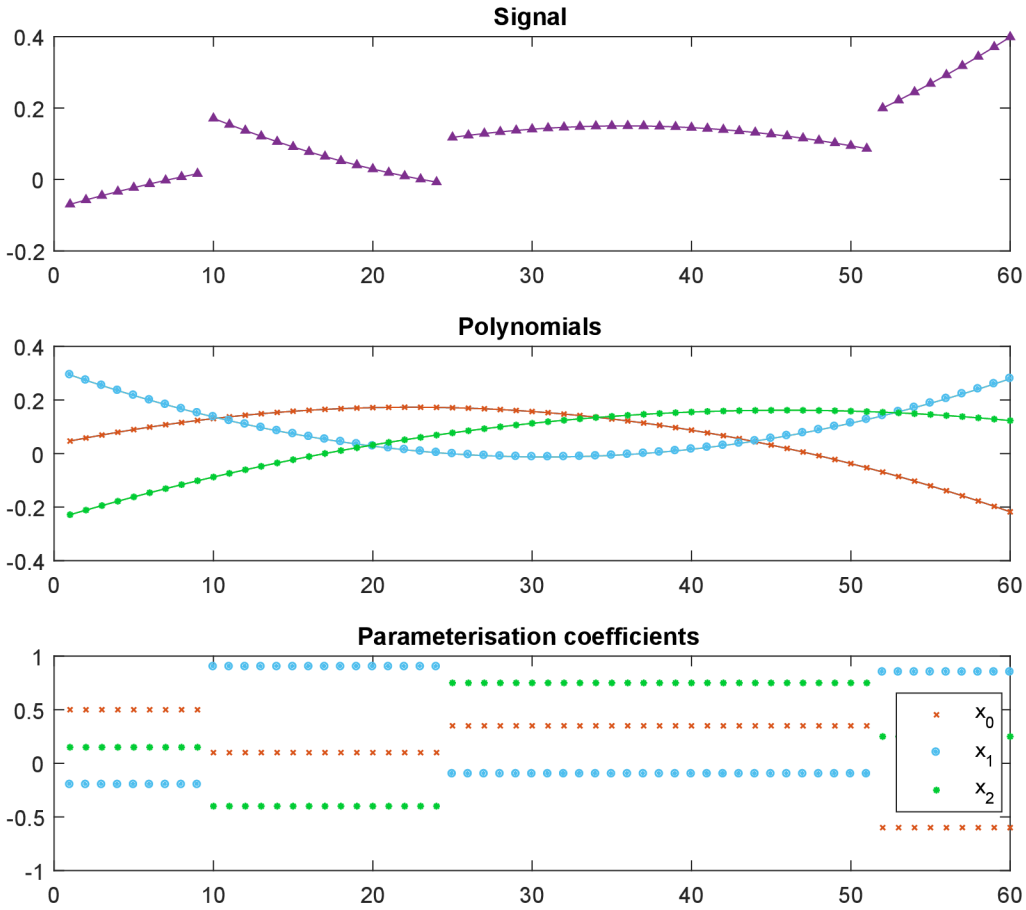

Fig. 3.3: Example of piecewise-quadratic signal parametrisation. The top plot shows the clean piecewise-quadratic signal $\mathbf{y}$ consisting of four segments. The middle plot shows three basis polynomials $\mathbf{p}_0, \mathbf{p}_1, \mathbf{p}_2$. The bottom plot shows the parametrisation coefficients $\mathbf{x}_0, \mathbf{x}_1, \mathbf{x}_2$.

Due to the facts described above, if $\mathbf{x}_k$ are piecewise-constant, the finite difference operator ∇ applied to vectors $\mathbf{x}_k$ produces sparse vectors $\nabla\mathbf{x}_k$, where each such a vector $\nabla\mathbf{x}_k$ has $S-1$ non-zeros at maximum. Moreover, the non-zero components of each $\nabla\mathbf{x}_k$ occupy the same

positions across $k = 0, \ldots, K$. Operator ∇ computes simple differences of each pair of adjacent elements in the vector, i.e. $\nabla\colon \mathbb{R}^N \to \mathbb{R}^{N-1}$ such that $\nabla\mathbf{z} = [z_2 - z_1, \ldots, z_N - z_{N-1}]^\top$.

Formulations mentioned above describe a clean polynomial signal without noise corruption. In the real world, it is usual that signals are corrupted by different types of noise. In this Thesis, it is assumed that the observed signal is corrupted by uncorrelated Gaussian noise with zero mean and non-zero variance. The definition of such a signal is

$$\mathbf{y} = \mathbf{P}\mathbf{x} + \mathbf{e}, \tag{3.3}$$

where $\mathbf{e}$ represents the noise vector of length N.

3.3 Concept of 1D signal segmentation and denoising

The general method for 1D signal segmentation and denoising can be defined and formally described by these main steps (illustrated in Fig. 3.4):

- Optimisation step using a proximal splitting algorithm,
- Segmentation and denoising,
  - Detection of segment borders (breakpoints),
  - Smoothing of detected segments.

Proposed methods differ from each other only in the first step (i.e. the optimisation step using a proximal splitting algorithm), specifically in the problem formulation and used proximal splitting algorithm.

Optimisation step using a proximal splitting algorithm

At first, the general recovery problem suitable for the solution of the 1D signal segmentation and denoising needs to be defined. The below-mentioned assumptions (which are based on the signal model description) are taken into account to formulate the general recovery problem:

- Observed signal $\mathbf{y}$ can be approximated by a linear combination of basis polynomials $\mathbf{p}_k$.
- The number of the signal segments S is considerably lower than the number of the signal samples N ($S \ll N$), which motivates to measure sparsity.
- Observed signal $\mathbf{y}$ is corrupted by Gaussian noise.

According to these assumptions, the general unconstrained recovery problem consists of two main terms: data fidelity term and penalisation term (penalty). General formulation of the recovery problem can be written as follows:

$$\hat{\mathbf{x}} = \arg\min_{\mathbf{x}} \; data\_fidelity\_term(\mathbf{x}) + penalization\_term(\mathbf{x}), \tag{3.4}$$

where $\mathbf{x}$ are parametrisation coefficients, and $\hat{\mathbf{x}}$ are the obtained parametrisation coefficients.

The proposed recovery problem is an optimisation program consisting of convex functions, which can be solved by using proximal splitting algorithms.

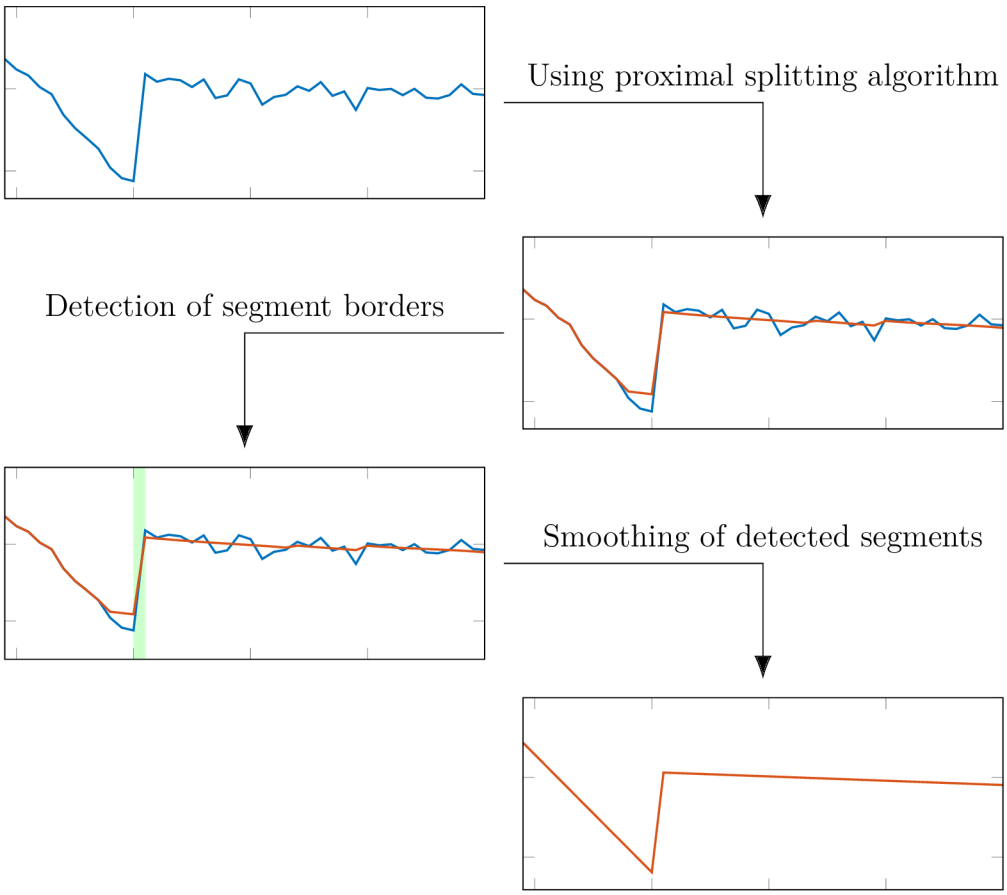

Fig. 3.4: Process of 1D signal segmentation. The diagram shows how the observed signal is processed during the 1D signal segmentation and denoising.

3.4 Formulated recovery problems

In this Thesis, several recovery problems suitable for the solution of the 1D signal segmentation/denoising process are proposed.

Recovery problem – Total variation According to the signal model description in Sec. 4.1, the number of the signal segments S is considerably lower than the number of the signal samples N, and the parametrisation coefficients $\mathbf{x}_k$ are piecewise-constant and positions of the breakpoints should be clearly identifiable in individual $\nabla\mathbf{x}_k$ – the non-zero values indicate the positions of segment borders. Estimation of such parametrisation coefficients $\hat{\mathbf{x}}$ of the observed signal $\mathbf{y}$ is needed. Then the breakpoints are found in estimated parametrisation coefficients $\hat{\mathbf{x}}$.

According to the above-mentioned assumptions, the following optimisation problem is formulated as

$$\hat{\mathbf{x}} = \arg\min_{\mathbf{x}} \|\nabla\mathbf{x}_0\|_0 + \cdots + \|\nabla\mathbf{x}_K\|_0 \quad \text{s.t.} \quad \|\mathbf{y} - \mathbf{P}\mathbf{x}\|_2 \leq \delta, \tag{3.5}$$

where $\mathbf{x}$ are parametrisation coefficients, $\hat{\mathbf{x}}$ are estimated parametrisation coefficients, ∇ is the difference operator, $\mathbf{y}$ is the observed signal, $\mathbf{P}$ is the matrix of basis polynomials and δ

is the parameter reflecting the noise level and model error. The functional $\|\cdot\|_0$ counts the non-zero elements of the vector. The $\|\nabla\cdot\|_0$ indicates the number of possible breakpoints in the vector.

The problem (3.5) is reformulated into its unconstrained form. Numerical solution of such unconstrained recovery problem using the Forward-backward and the Douglas–Rachford algorithms was presented in our paper [25].

The proposed experiments showed that the denoising process is better when the FB algorithm is used. However, the DR algorithm obtained a better breakpoint detection than the FB algorithm.

Recovery problem – ℓ_{21}-norm The presented recovery problem (3.5) from Sec. 3.4 does not ensure finding the possible breakpoint candidates at the same positions across all difference vectors $\nabla\hat{\mathbf{x}}_k$ because that approach utilises $\|\nabla\cdot\|_0$ to treat each $\mathbf{x}_k$ separately. Therefore, the correct breakpoints could be discarded by this approach. To avoid this phenomenon, the ℓ_{21}-norm [26] was used to enforce joint breakpoints over across all the difference vectors $\nabla\mathbf{x}_k$ in the following optimisation problem:

$$\hat{\mathbf{x}} = \arg\min_{\mathbf{x}} \ \|[\tau_0\nabla\mathbf{x}_0,\ldots,\tau_K\nabla\mathbf{x}_K]\|_{21} \ \text{ s.t. } \|\mathbf{y}-\mathbf{P}\mathbf{x}\|_2 \leq \delta, \tag{3.6}$$

where $\mathbf{x}$ are parametrisation coefficients, $\hat{\mathbf{x}}$ are estimated parametrisation coefficients, ∇ is the difference operator, τ_k are $K+1$ positive regularisation weights, corresponding to the individual polynomial degrees, $\|\cdot\|_{21}$ indicates the ℓ_{21}-norm, $\mathbf{y}$ is the observed signal, $\mathbf{P}$ is the matrix of basis polynomials, and δ is the parameter reflecting the noise level and model error.

The recovery problem (3.6) is reformulated to the unconstrained form and the numerical solution using the Forward-backward based primal-dual algorithm and the Chambolle–Pock algorithm was presented in our paper [27] and article [28].

The proposed experiments showed that for both denoising and breakpoint detection, the FBB-PD algorithm gave better results than the CP algorithm. The comparison of the FBB-PD algorithm with the FB algorithm revealed that the FBB-PD algorithm provided better results in all areas.

Recovery problem – imitation of non-convexity Another way how the breakpoint detection could be improved is the imitation of non-convexity. To enhance the sparsity of the solution, it is possible to imitate the non-convexity via a series of convex programs. This approach is not new in general, it has been both theoretically and practically justified in [29], for example. Such a series of convex problems is formulated such that the parameters of the currently solved convex problem depend on the solution of the latest problem. The optimisation problem that extends problem (3.6) from previous section by the change of parameters can be formulated as follows:

$$\hat{\mathbf{x}}^{(j)} = \arg\min_{\mathbf{x}} \|\text{reshape}(L^{(j)}\mathbf{x})\|_{21} \text{ s.t. } \|\mathbf{y}-\mathbf{P}\mathbf{x}\|_2 \leq \delta, \tag{3.7}$$

where the linear operator $L^{(j)}$ includes parameters, which change with each problem repetition, where $j = 0, \ldots, J$ represents the counter for problem repetitions, $\hat{\mathbf{x}}^{(j)}$ are estimated parametrisation coefficients, $\mathbf{x}$ are parametrisation coefficients, $\mathbf{y}$ is the input signal, $\mathbf{P}$ is the matrix of polynomials, δ is the parameter reflecting the noise level and model error, and reshape() operator takes the stacked vector $L^{(j)}\mathbf{x}$ to the form of a matrix with disjoint columns.

After a defined number of inner iteration (IT) of the proximal splitting algorithm, the parameters in the operator $L^{(j)}$ are recomputed. Therefore, the process of re-computation is called re-weighting in this Thesis.

Numerical solution to the unconstrained form of the optimisation problem (3.7) using non-weighted and re-weighted variants of the Condat algorithm was presented in our paper[30].

The proposed experiments showed that for both breakpoint detection and denoising, the non-weighted Condat algorithm gave better results than re-weighted Condat algorithm.

Testing different types of bases In the previous sections, the modified standard basis $\mathbf{S}$ was used in all experiments. The disadvantage of using the modified standard basis is that it is necessary to set the regularisation weights for the individual polynomials of the basis, because the influence of the individual polynomials on the segmentation process is not equal and the achieved results are worse without weighting.

The aim of this section is to reduce the number of tunable parameters caused by using the modified standard basis. Therefore, different types of bases introduced in Sec. 3.1 will be exploited, which will avoid the weighting of basis polynomials.

This approach was already presented in our article [31], where it is demonstrated that using another types of bases is a promising way how to improve the segmentation results of the non-weighted Condat algorithm. The paper shows that the best results are achieved with R-bases and O-bases. Therefore, the experiments in this section will be performed only for these two types of bases.

The optimisation problem for this section is identical as in Sections 3.4 and 3.4and is formulated as follows:

$$\hat{\mathbf{x}} = \arg\min_{\mathbf{x}} \|\text{reshape}(L\mathbf{x})\|_{21} \text{ s.t. } \|\mathbf{y} - \mathbf{P}\mathbf{x}\|_2 \leq \delta, \tag{3.8}$$

where L is a linear operator, $\hat{\mathbf{x}}$ are estimated parametrisation coefficients, $\mathbf{x}$ are parametrisation coefficients, $\mathbf{y}$ is input signal, $\mathbf{P}$ is the matrix of polynomials, δ is the parameter reflecting the noise level and model error, and reshape() operator takes the stacked vector $L^{(j)}\mathbf{x}$ to the form of a matrix with disjoint columns.

The unconstrained form of the optimisation problem (3.8) is solved using Forward-backward based primal-dual (FBB-PD) algorithm and the non-weighted Condat algorithm.

The performed experiments showed that from the breakpoint detection point of view, the non-weighted Condat algorithm gave better results than the FBB-PD algorithm for both O- and R-bases. The results showed that the standard modified basis performed the best for linear signals and R-bases were the best for quadratic signals.

4 EDGE DETECTION IN IMAGES

4.1 Signal model description

The 2D signal model used in this Thesis is a natural extension of the 1D signal model described in Sec. 4.1. Therefore, the images are assumed to consist of non-overlapping piecewise-polynomial patches. The edges in the image represent positions where the adjacent patches (segments) change their polynomial characterisation. Within the patches (segments), the respective representation stays steady.

Let the 2D signal (image) $\mathbf{Y} \in \mathbb{R}^{M \times N}$ contain entries $Y[m, n]$, $m = 1, \ldots, M$, $n = 1, \ldots, N$. The image is modelled in the similar way as the 1D signal (see Eq. (**??**))

$$\mathbf{Y} = \bar{\mathbf{P}}_{00} \odot \mathbf{X}_{00} + \bar{\mathbf{P}}_{01} \odot \mathbf{X}_{01} + \cdots + \bar{\mathbf{P}}_{KK} \odot \mathbf{X}_{KK}, \tag{4.1}$$

where $\mathbf{X}_{kl}$ are matrices of parametrisation coefficients of the size $M \times N$, and $\bar{\mathbf{P}}_{kl}$ are basis images of size $M \times N$ as defined below in Eq. (4.2).

The image $\mathbf{Y}$ is assumed to be piecewise-polynomial and consists of S independent patches (segments). Each patch $s \in \{1, \ldots, S\}$ is described by $(K+1)^2$ basis polynomial images $\mathbf{P}_{kl}$. Matrices $\mathbf{X}_{kl}$ are assumed to be piecewise-constant within the particular patches, with the change at the patch borders.

For the images, the polynomial basis images $\bar{\mathbf{P}}_{kl} \in \mathbb{R}^{M \times N}$ are needed instead of the polynomial vectors $\mathbf{p}_k$. The extension from the polynomial vectors to the polynomial basis images is done through the Kronecker product of 1D polynomial vectors $\mathbf{p}_{k\mathrm{v}} \in \mathbb{R}^N$ and $\mathbf{p}_{l\mathrm{h}} \in \mathbb{R}^M$, where the subscripts "v" and "h" represent the vertical and the horizontal directions of the 1D polynomial vectors, respectively. And the subscripts "k" and "l" represent the degree of the vertical and horizontal polynomials, respectively. Note that for the definition of the 2D signal model, the degrees of the polynomials in the vertical and the horizontal direction are supposed to be identical, i.e. K.

The set of basis 2D polynomials are formed by all the combinations of $\mathbf{p}_{k\mathrm{v}}$ and $\mathbf{p}_{l\mathrm{h}}$, where $k = 0, \ldots, K$ and $l = 0, \ldots, K$ such that

$$\begin{aligned} \bar{\mathbf{P}}_{00} &= \mathbf{p}_{0\mathrm{v}} \cdot \mathbf{p}_{0\mathrm{h}}^\top \\ \bar{\mathbf{P}}_{01} &= \mathbf{p}_{0\mathrm{v}} \cdot \mathbf{p}_{1\mathrm{h}}^\top \\ &\vdots \\ \bar{\mathbf{P}}_{KK} &= \mathbf{p}_{K\mathrm{v}} \cdot \mathbf{p}_{K\mathrm{h}}^\top \end{aligned} \tag{4.2}$$

making altogether $(K+1)^2$ polynomial basis images. When both the vertical and horizontal polynomial vectors form the respective 1D orthonormal bases, the new generated polynomial basis images form the 2D orthonormal basis.

Also, the 2D signal model can be expressed as a matrix-vector multiplication

$$\begin{aligned}\mathbf{y} = \mathbf{P}\mathbf{x} &= [\mathbf{P}_{00} \mid \cdots \mid \mathbf{P}_{KK}] \begin{bmatrix} \mathbf{x}_{00} \\ \hline \vdots \\ \hline \mathbf{x}_{KK} \end{bmatrix} \\ &= \left[\operatorname{diag}(\operatorname{vec}(\bar{\mathbf{P}}_{00})) \mid \cdots \mid \operatorname{diag}(\operatorname{vec}(\bar{\mathbf{P}}_{KK}))\right] \begin{bmatrix} \operatorname{vec}(\mathbf{X}_{00}) \\ \hline \vdots \\ \hline \operatorname{vec}(\mathbf{X}_{KK}) \end{bmatrix},\end{aligned} \tag{4.3}$$

where $\mathbf{y} \in \mathbb{R}^{MN}$, $\mathbf{P} \in \mathbb{R}^{MN \times (K+1)^2 MN}$, $\mathbf{x} \in \mathbb{R}^{(K+1)^2 MN}$, and $\operatorname{vec}(\cdot)$ is the vectorisation operator, which stacks the image columns, one after another, into a single column.

Vectors $\mathbf{x}_{kl}$ are assumed to be piecewise-constant. The finite difference operator ∇ applied to them produces sparse vectors $\nabla\mathbf{x}_{kl}$ with non-zero components occupying the same positions across $k = 0, \ldots, K$ and $l = 0, \ldots, K$.

The definition of an image corrupted by uncorrelated Gaussian noise with zero mean and non-zero variance is

$$\mathbf{y} = \mathbf{P}\mathbf{x} + \operatorname{vec}(\mathbf{E}), \tag{4.4}$$

where $\mathbf{E}$ represents the noise matrix of size $M \times N$.

4.2 Concept of image edge detection

Concept of the image edge detection is divided into two main steps, similar to the 1D signal segmentation and denoising process, except the last step "Smoothing of detected segments", which is not utilised in proposed image edge detection method:

- Optimisation using a proximal splitting algorithm,
- Edge identification.

Since vectorised images are used for the process of the image edge detection, the illustration in Fig. 3.4 demonstrates the individual steps of both 1D and 2D process (except the last step "Smoothing of detected segments").

4.3 Recovery problem and algorithm used

Since it is assumed that the clean image consists of several non-overlapping polynomial patches, the piecewise-constant parametrisation coefficients $\{\mathbf{x}_{k\ell}\}_{k,\ell}$, which are sparse under the difference operator ∇, can be found. The image consists of edges with different orientations. To successfully detect the edges in the image, it is necessary to seek the edges in at least two perpendicular directions (usually the vertical and horizontal direction). Therefore, two forms

of the difference operator are used – the horizontal and the vertical one. As mentioned before, the analysed image is supposed to be corrupted by an i.i.d. Gaussian noise.

These assumptions lead to the following formulation of the constrained optimisation problem

$$\hat{\mathbf{x}} \;=\; \arg\min_{\mathbf{x}} \left\{ \|\operatorname*{reshape}_{\mathrm{v}}(L_{\mathrm{v}}\mathbf{x})\|_{21} + \lambda \|\operatorname*{reshape}_{\mathrm{h}}(L_{\mathrm{h}}\mathcal{M}(\mathbf{x}))\|_{21} \right\} \text{ s.t. } \|\mathbf{y} - \mathbf{P}\mathbf{x}\|_2 \;\leq\; \delta, \quad (4.5)$$

where the vector $\hat{\mathbf{x}}$ represents the obtained optimal parametrisation coefficients, $\mathbf{y}$ is the vectorised image $\mathbf{Y}$, $\mathbf{x}$ are the vectorised parametrisation coefficients $\mathbf{X}$, and $\mathbf{P}$ is a matrix of polynomial bases images. The parameter δ reflects the noise level and the model imperfections.

Numerical solution of the unconstrained form of the optimisation problem (4.5) using the Condat algorithm was presented in our paper [32].

4.4 Image dataset and bases, evaluation

Natural images For the experiments, the Berkeley Segmentation Data Set and Benchmarks 500 (BSDS500) [33] is used. This dataset consists of 500 natural RGB images $\mathbf{Y}_{\mathrm{RGB}}$. Each image of the BSDS500 dataset was manually annotated on average by five different subjects (see some examples of the natural images and their annotations in Fig. 4.1). Further information on how the annotations were taken can be found in [34]. The BSDS500 is divided into 3 groups: 200 train images, 100 images for validation, and 200 test images. BSDS500 with its human annotations serves as the ground truth for comparing different segmentation and edge detection methods.

Fig. 4.1: Example of RGB natural image of BSDS500 dataset with its annotations by humans.

For the testing, also the Berkeley Segmentation Data Set and Benchmarks 300 (BSDS300) [33] is used. This dataset consists of 300 natural RGB images $\mathbf{Y}_{\mathrm{RGB}}$, and is divided into 2 groups: 200 train images, 100 test images. The train subset of BSDS300 is equal to the train subset of BSDS500 and the test subset of BSDS300 is same as the validation subset of BSDS500.

Types of processed images For the purpose of this Thesis, three groups of real images $\mathbf{Y} \in \mathbb{R}^{M \times N}$ are used. The first group of images consists of the set of RGB images denoted as $\mathbf{Y}_{\mathrm{RGB}}$. The second group of images consists of the grayscale images $\mathbf{Y}_{\mathrm{gray}}$, which were obtained from the first group of RGB images by converting the RGB image to the grayscale

image. For the conversion, the Matlab function "rgb2gray" was used. By converting, the hue and saturation information are eliminated while the luminance is retained.

The third group is formed with noisy grayscale images $\mathbf{Y}_{\text{noisy}}$. The Gaussian i.i.d. noise $\mathbf{E}$ is added to the grayscale images $\mathbf{Y}_{\text{gray}}$, resulting in grayscale noisy images $\mathbf{Y}_{\text{noisy}}$, such that

$$\mathbf{Y}_{\text{noisy}} = \mathbf{Y}_{\text{gray}} + \mathbf{E}, \quad \mathbf{E} \sim \mathrm{N}(\mathbf{0}, \sigma_{\mathrm{E}}^2). \tag{4.6}$$

Bases For the experiments, the basis consisting of the $(K+1)^2$ basis images, where $K = 2$, is used. The generation process of polynomial basis images is defined in Eq. (4.2) and it is independent of the particular choice of the basis type.

A standard basis $\bar{\mathbf{S}}$, which was generated using the polynomials of the modified standard basis $\mathbf{S}$ using Eq. (4.2). See Fig. 4.2 for examples of standard basis images of $\bar{\mathbf{S}}$.

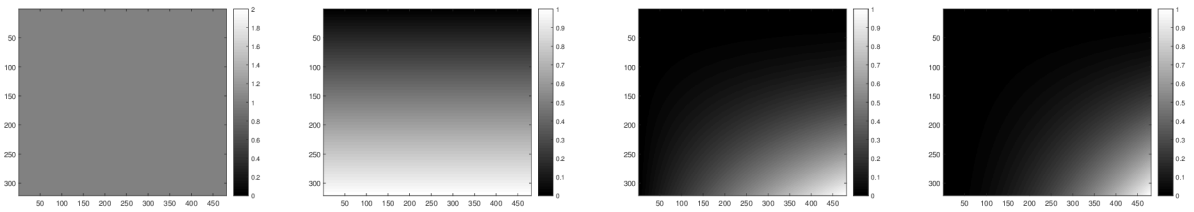

Fig. 4.2: Examples of polynomial images $\bar{\mathbf{S}}_{00}$, $\bar{\mathbf{S}}_{01}$, $\bar{\mathbf{S}}_{12}$, $\bar{\mathbf{S}}_{22}$ of size 321×481, generated from the 1D modified standard basis $\mathbf{S}$ of degree $K = 2$.

4.5 Evaluation

The datasets of natural images with human annotations of image edges/segments are used for the evaluation of the edge detection accuracy and for the comparison of the results of different algorithms.

For evaluation of the edge detection accuracy, the precision–recall curve and F-measure score [34] are used. The parametric curve reflects the relation between the precision and the recall for changing threshold value of the edge detector.

Precision (P) is defined as a ratio of true positive (TP) detections to the sum of false positive (FP) and true positive (TP) detections: $\mathrm{P} = \frac{\mathrm{TP}}{\mathrm{FP}+\mathrm{TP}}$.

Recall (R) is defined as a ratio of true positive (TP) detections to the sum of false negative (FN) and true positive (TP) detections: $\mathrm{R} = \frac{\mathrm{TP}}{\mathrm{FN}+\mathrm{TP}}$.

F-measure score (F) is defined as a harmonic mean of precision and recall:

$$\mathrm{F} = 2\frac{\mathrm{P} \cdot \mathrm{R}}{\mathrm{P} + \mathrm{R}}. \tag{4.7}$$

The optimal threshold value of the detector gives the maximal F-measure score along the curve.

4.6 Experiments

The image edge detection method presented in this Thesis is tuned only on the train and validation groups of images. During the training and validation phase, the optimal values of parameter δ are chosen for both RGB and grayscale images. Since the proposed approach is applied to each colour channel separately, the best merging approach is also chosen. These values of parameter δ and the best merging approach for RGB images are then used in the test phase. The final evaluation is performed on the test group of images. Example of edge detection result on RGB and grayscale test images is displayed in Fig. 4.3.

Fig. 4.3: Examples of edge detection results for RGB and grayscale image of BSDS500 test subset. From the left: original colour image, detected edges in RGB image, grayscale image, detected edges in grayscale image.

The precision–recall curves of other approaches are displayed in Fig. 4.4 on the left side. The proposed image edge detection method for both grayscale and RGB test images gives better results in term of F-measure score than the classical gradient-based edge detection techniques (Prewitt, Sobel, and Roberts) and Laplacian of Gaussian.

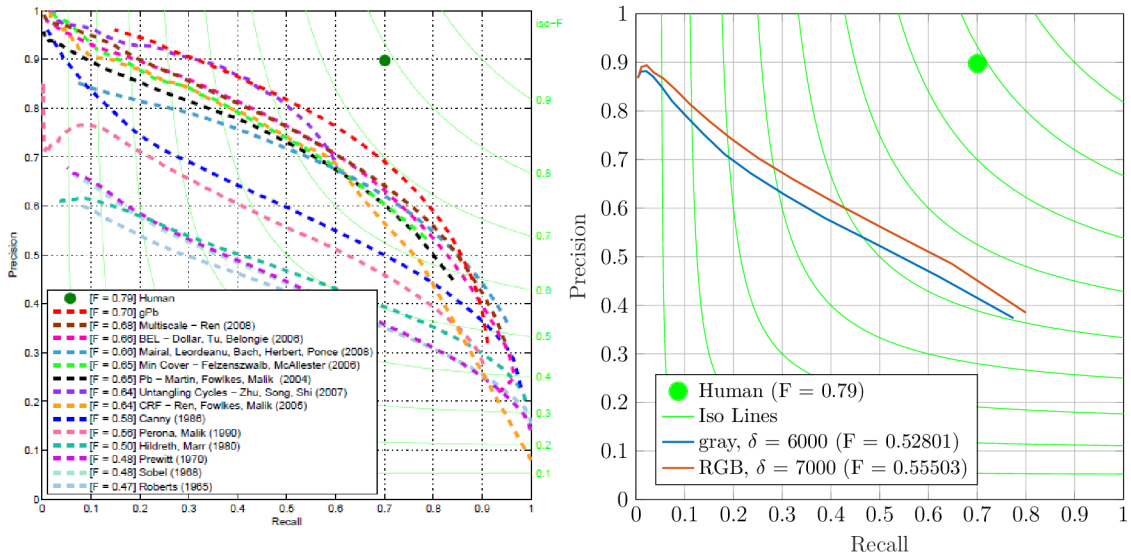

Fig. 4.4: Precision–recall curves with their maximum F-measure scores for δ settings. The precision–recall curves of other approaches described are displayed on the left side. The precision–recall curves of proposed approach for RGB and grayscale images are plotted on the right side. Presented results are for test subset of BSDS300 consisting of 100 natural images.

CONCLUSION

This Thesis dealt with breakpoint/edge detection in 1D and 2D signals using sparse signal representation and convex optimisation. The main objective of this Thesis was to provide a novel method for detecting edges in an image. Several suitable approaches were selected and tested on 1D signals and the best of them was subsequently extended to 2D. The Thesis was divided into main three parts.

The first part included a basic overview, the notation used and explained sparse signal representation and convex optimisation, including proximal splitting algorithms, which were implemented in this Thesis. Then here is presented a discussion of a selection of topics from the field of image processing that were relevant to this Thesis. This included image segmentation, edge detection and enhancement, and denoising. And finally, it gave an overview of the edge detection methods used.

The second part focused on finding the most promising algorithm for breakpoint detection in a 1D signal, which was then extended for the use in 2D. In this part, the input data (test signals, polynomial bases), formulation of the signal model and the general concept for the 1D signal segmentation and denoising were introduced, several possible solutions were designed, and the experiments and their results were evaluated from two perspectives – the quality evaluation of segmentation and denoising. A general concept of the proposed 1D signal segmentation process explained the basic idea of the proposed methodology. The general method was divided into two main steps – "Optimisation step using a proximal splitting algorithm" and "Segmentation and denoising step". The methods proposed in the second part differed from each other only in the first step, namely in the particular formulation of the problem and in the proximal splitting algorithm that was used.

First, an ℓ_1-based unconstrained formulation of the recovery problem using the total variation was proposed, and two proximal algorithms (the Forward-backward (FB) and the Douglas–Rachford (DR) algorithm) were used to solve this recovery problem. The carried experiments revealed that the denoising process is better when the FB algorithm is used. However, the DR algorithm obtained a better breakpoint detection than the FB algorithm. Considering that noise reduction was only a by-product of the proposed algorithm, performance in breakpoint detection were more important.

Since the total variation treated each parametrisation vector separately, it did not ensure that possible breakpoint candidates were found at the same positions across all difference vectors. Therefore, the correct breakpoints could be discarded by this approach. To avoid this phenomenon, the ℓ_{21}-norm was used to enforce joint breakpoints over the difference vectors. The second recovery problem using ℓ_{21}-norm was solved using the Forward-backward based primal-dual (FBB-PD) and the Chambolle–Pock (CP) algorithm. For both denoising and breakpoint detection, the FBB-PD algorithm gave better results than the CP algorithm. The comparison of the FBB-PD algorithm with the FB algorithm revealed that the FBB-PD algorithm provided better results in all areas. Based on these results, a conclusion can be made that the use of the ℓ_{21}-norm has led to a significant improvement in the results, compared to

the simple total variation-based approach.

Another idea to improve the breakpoint detection was to imitate non-convexity via a series of convex programs, where the parameter of the currently solved convex problem depended on the latest solution. In this sense, the extended ℓ_{21}-norm based unconstrained recovery problem was defined, and it was solved using the re-weighted and non-weighted variants of the Condat algorithm. The comparison of the non-weighted and re-weighted Condat algorithms showed that the breakpoint detection and denoising was better when the non-weighted Condat algorithm was used. Thus, there was no confirmation that the imitation of non-convexity would bring an improvement in the detection of breakpoints. Compared to the FBB-PD algorithm, the non-weighted Condat algorithm achieved worse results in the breakpoint detection and denoising. The differences between FBB-PD and the non-weighted Condat algorithm were not so significant for the signals with big jump heights and high SNR.

The last experiments from the second part focused on the use of different types of bases, specifically O- and R- bases, in contrast to previous experiments where a modified standard S-basis was used. The ℓ_{21}-norm based recovery problem was used and the FBB-PD and the non-weighted Condat algorithms were used to solve it. From the comparison between the FBB-PD algorithm and the non-weighted Condat algorithm, it appeared that it was advantageous to use the FBB-PD algorithm. However, for solving the task in more dimensions, the non-weighted Condat algorithm offers a better possibility. From the breakpoint detection point of view, it was evaluated that the non-weighted Condat algorithm gave better results than the FBB-PD algorithm for both O- and R-bases. The results showed that the standard modified basis performed the best for linear signals and R-bases were the best for quadratic signals.

The third part of the Thesis dealt with edge detection in images. First, 2D signal model is formulated, then the general concept of the proposed image edge detection is introduced, followed by the presentation of the image dataset and the evaluation metric used, and finally, by the description of the specific image edge detection solution, including experiments and their evaluation. A comparison with other edge detection approaches was also included in this part. The general concept of image edge detection, was divided into two main steps – "Optimisation step using a proximal splitting algorithm" and "Edge identification".

For the experiments, 2D polynomial bases and the natural image datasets BSDS500 and BSDS300 (Berkeley Segmentation Data Set) are needed. These datasets are often used for the comparison of segmentation and edge detection methods containing manually annotated image edges/segments used as the ground truth. The BSDS500 dataset is divided into three classes: train, validation, and test subset, and the BSDS300 is only a subset of the BSDS500 containing only images from the train and validation subsets. To evaluate the accuracy of the edge detection, the precision–recall curve and the F-measure score were used.

The extended ℓ_{21}-norm based recovery problem for the use with 2D signals was presented. A suitable algorithm for solving the defined recovery problem seemed to be the non-weighted Condat algorithm, which obtained the most promising results when used on 1D signals.

First, the experiments on grayscale and colour images from the train and validation subsets

of the BSDS500 dataset were done. For the purpose of these experiments a standard modified basis was chosen. The experiments were divided into two phases – a training phase and a validation phase. The output of the proposed edge detection method was compared with the image annotation from the BSDS500 dataset.

In the training phase, several values of parameter δ were tested. The output of the training phase was the δ with the highest F-measure score (for both grayscale and RGB images). In the case of RGB images, the image edge detection algorithm was applied to each colour channel separately. It was necessary to compose the outputs of the channels into one output. Therefore, four merging approaches were proposed, and the best merging method was selected for the other experiments. The purpose of the validation phase was to refine the parameter δ settings, where the steps between the tested values of parameter δ were smaller than in the training phase. The δ parameter with the highest F-measure scores was identified as the optimal setting for the testing phase.

The proposed edge detection method was compared with several other algorithms. The comparison was made on the test subset of the public datasets BSDS300 and BSDS500. The edge detection method obtained better results for RGB images than for its grayscale variants. Our proposed method (for both RGB and grayscale images) obtained better results on the BSDS300 dataset than the classical gradient-based edge detection techniques (Prewitt, Sobel, and Roberts) and the Laplacian of Gaussian, whose output is a raw edge detection. Considering that our proposed approach did not involve any post-processing, the results obtained were very good in terms of the raw edge detection. All methods that performed better than the proposed approach included some post-processing, or were much more sophisticated. Considering that the more sophisticated methods require some initial estimation of edges (raw edge detection) their results could be even better when combined with our proposed method. The method was also tested on the BSDS500 dataset, where it gave slightly better results on RGB images than the Canny detector, which includes post-processing.

The aim of the last experiments of the third part was to find out how our proposed method copes with edge detection on noisy grayscale images with varying levels of noise. The results showed that on less noisy images (SNR $\in \{25, 30, 35\}$), the method gave almost the same results, according to the F-measure score, as when used on "clean" images.

Other ideas and possible directions for future research can be considered. Decomposing the image into LAB channels instead of RGB channels could be a possible approach to improve edge detection in colour images. Furthermore, the input data for the "Optimisation using proximal splitting algorithm" step could be not only intensity images but also parametric maps. The resulting outputs could then be combined with the outputs from the individual colour channels. Moreover, the coupling of the colour channels can be already incorporated into the recovery problem [35, Chapter 6], instead of applying the proposed method to each colour channel separately. As a final direction for future development, the extension of the proposed method by post-processing to produce compact, thin edges can be considered.

REFERENCES

[11] R. Giryes, M. Elad, and A. M. Bruckstein. Sparsity based methods for overparameterized variational problems. *SIAM Journal on Imaging Sciences*, 8(3):2133–2159, 2015.

[12] J. M. Giron-Sierra. *Sparse Representations*, pages 151–261. Springer Singapore, Singapore, 2017.

[13] P. Rajmic and M. Danková. *Úvod do rídkých reprezentací signálu a komprimovaného snímání*. Vysoké ucení technické v Brne, 2014.

[14] M. Elad. *Sparse and Redundant Representations: From Theory to Applications in Signal and Image Processing*. Springer, 1st edition, 2010.

[15] Z. Zhang, Y. Xu, J. Yang, X. Li, and D. Zhang. A survey of sparse representation: Algorithms and applications. *IEEE Access*, 3:490–530, 2015.

[16] S. P. Boyd and L. Vandenberghe. *Convex Optimization*. Cambridge University Press, 2004.

[17] P. Combettes and J. Pesquet. Proximal splitting methods in signal processing. *Fixed-Point Algorithms for Inverse Problems in Science and Engineering*, 49:185–212, 2011.

[18] A. Chambolle and T. Pock. A first-order primal-dual algorithm for convex problems with applications to imaging. *Journal of Mathematical Imaging and Vision*, 40(1):120–145, 2011.

[19] N. Komodakis and J. Pesquet. Playing with duality: An overview of recent primal-dual approaches for solving large-scale optimization problems. *IEEE Signal Processing Magazine*, 32(6):31–54, 2015.

[20] L. Condat. A generic proximal algorithm for convex optimization—application to total variation minimization. *IEEE Signal Processing Letters*, 21(8):985–989, 2014.

[21] L. Condat. A primal-dual splitting method for convex optimization involving Lipschitzian, proximable and linear composite terms. *Journal of Optimization Theory and Applications*, 158(2):460–479, 2013.

[22] J. Jan. *Medical Image Processing, Reconstruction and Restoration: Concepts and Methods*. CRC Press, 1st edition, 2005.

[23] W. Burger and M. Burge. *Principles of Digital Image Processing: Fundamental Techniques*. Springer London, 2010.

[24] N. Perraudin, D. I. Shuman, G. Puy, and P. Vandergheynst. UNLocBoX: A MATLAB convex optimization toolbox using proximal splitting methods. 2014, arXiv: 1402.0779.

[25] P. Rajmic and M. Novosadová. On the limitation of convex optimization for sparse signal segmentation. In *2016 39th International Conference on Telecommunications and Signal Processing (TSP)*, pages 550–554, Vienna, Austria, June 2016.

[26] M. Kowalski and B. Torrésani. Structured Sparsity: from Mixed Norms to Structured Shrinkage. In *Signal Processing with Adaptive Sparse Structured Representations (SPARS'09)*, pages 1–6, 2009.

[27] M. Novosadová and P. Rajmic. Piecewise-polynomial curve fitting using group sparsity. In *2016 8th International Congress on Ultra Modern Telecommunications and Control Systems and Workshops (ICUMT)*, pages 320–325, Lisbon, Portugal, Oct. 2016.

[28] P. Rajmic, M. Novosadová, and M. Danková. Piecewise-polynomial signal segmentation using convex optimization. *Kybernetika*, 53(6):1131–1149, Dec. 2017.

[29] E. J. Candes, M. B. Wakin, and S. P. Boyd. Enhancing sparsity by reweighted ℓ_1 minimization. *Journal of Fourier Analysis and Applications*, 14:877–905, 2008.

[30] M. Novosadová and P. Rajmic. Piecewise-polynomial signal segmentation using reweighted convex optimization. In *2017 40th International Conference on Telecommunications and Signal Processing (TSP)*, pages 769–774, Barcelona, Spain, 2017.

[31] M. Novosadová, P. Rajmic, and M. Šorel. Orthogonality is superiority in piecewise-polynomial signal segmentation and denoising. *EURASIP Journal on Advances in Signal Processing*, 2019(6):1–15, Jan. 2019.

[32] M. Novosadová and P. Rajmic. Image edges resolved well when using an overcomplete piecewise-polynomial model. In *2018 12th International Conference on Signal Processing and Communication Systems (ICSPCS)*, pages 1–10, Cairns, QLD, Australia, Dec. 2018.

[33] P. Arbeláez, M. Maire, C. Fowlkes, and J. Malik. Contour detection and hierarchical image segmentation. *IEEE Transactions on Pattern Analysis and Machine Intelligence*, 33(5):898–916, 2011.

[34] D. Martin, C. Fowlkes, and J. Malik. Learning to detect natural image boundaries using local brightness, color, and texture cues. *IEEE Transactions on Pattern Analysis and Machine Intelligence*, 26(5):530–549, 2004.

[35] D. L. Kristian Bredies. *Mathematical Image Processing*. Birkhäuser Cham, 2019.

Curriculum Vitæ

Michaela Novosadová

Contact

E-mail:	micha.novosadova@gmail.com
WWW:	`https://www.vut.cz/lide/michaela-novosadova-125066`

QUALIFICATION AND PROFESSIONAL CAREER

Qualification

2014 – 2023 (planned)	Ph.D. in Teleinformatics, Brno University of Technology, Faculty of Electrical Engineering and Communication. Doctoral thesis: *Image edge detection using convex optimisation*
2012 – 2014	MSc. in Biomedical Engineering and Bioinformatics, Brno University of Technology, Faculty of Electrical Engineering and Communication, Master's thesis: *Segmentation of 3D image data using advanced textural and shape features*
2009 – 2012	BSc. in Biomedical Technology and Bioinformatics, Brno University of Technology, Faculty of Electrical Engineering and Communication, Bachelor's thesis: *Automatic segmentation of regions of interest in a human vertebra*

Professional career

2020 – present	Order manager at TESCAN Medical, s.r.o.
2018 – 2020	Research and development professional at TESCAN Medical, s.r.o.
2016 – 2018	Junior researcher at the Brno University of Technology
2015 – 2018	Research and development professional at 3Dim Laboratory, s.r.o.
2014 – 2015	Coordinator at The International Clinical Research Center of St. Anne's University Hospital in Brno

RESEARCH PROJECTS

2017 – 2020	FEKT-S-17-4476 Multimodální zpracování nestrukturovaných dat s využitím strojového učení a sofistikovaných metod analýzy signálů a obrazů
2016 – 2018	GA16-13830S Perfuzní zobrazování v magnetické rezonanci pomocí komprimovaného snímání

OTHER QUALIFICATIONS AND KNOWLEDGE

Language knowledge	Czech language (native speaker)
	English language (level B2)
	German language (level B1)

Awards

June 2014	Master's degree with honors
June 2014	Dean's award for outstanding Master's thesis
June 2012	Bachelor's degree with honors

SUMMARY OF PUBLICATION ACTIVITIES

- Scientific journals with impact factor according to Web of Science: 2
- International conferences indexed in Web of Science or Scopus: 5
- Total number of citations according to Web of Science: 23
- Total number of citations according to Scopus: 31
- H-index according to Web of Science: 3
- H-index according to Scopus: 4
- Number of released products: 1

ABSTRACT

Image edge detection is one of the most important techniques in digital image processing. It is used, among other things, as the first step of image segmentation. Therefore, it remains an area of interest for researchers trying to develop ever-better detection approaches. The main objective of this Thesis is to find a suitable method for image edge detection using convex optimisation. The proposed method is based on sparse modelling, and its main part is formulated as a convex optimisation problem solved by proximal algorithms. For defining the optimisation problem, it is assumed that the signal can be modelled as an over-parameterised, piecewise-polynomial signal that consists of disjoint segments. The number of these segments is significantly smaller than the number of signal samples, thereby encouraging the use of sparsity. The formulation of a suitable optimisation problem is first performed on one-dimensional signals since the implementation and comparison of the different algorithms is significantly easier and less time-consuming for one-dimensional signals than two-dimensional ones.

The first part of the Thesis introduces the basic theory in signal processing, sparsity, convex optimisation and proximal algorithms. It also presents a cross-section of the methods used for image edge detection. The second part of the Thesis focuses on the formulation and the subsequent evaluation of individual optimisation problems for the segmentation of one-dimensional synthetic signals corrupted by noise. The evaluation is conducted in terms of both denoising and breakpoint detection accuracy. The last part of the Thesis is dedicated to expanding the best-performing approach for breakpoint detection in one-dimensional signals for the application to image edge detection. The proposed approach is tested on a standardised dataset of images containing manually labelled edges of several subjects. The results of the proposed method are evaluated using precision-recall curves and their maximum F-measure score, and then compared with other edge detection methods.